

## ***Comparison the performance of both CuO and La<sub>2</sub>O<sub>3</sub> as a metal oxide nanoparticles Catalyst in the carbonylation the Glycerol with Carbone Dioxide to produce Glycerol carbonate.***

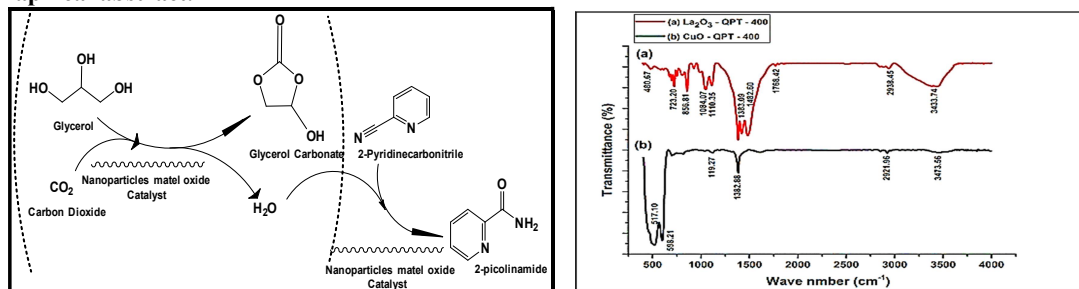
Jassim Mohamed Hamed Al- Kurdhani <sup>a, c</sup>, Huajun Wang <sup>a, b, \*</sup>, Xiong Zhou <sup>a</sup>.

<sup>a</sup> Key Laboratory for Material Chemistry for Energy Conversion and Storage, Ministry of Education, School of Chemistry and Chemical Engineering, Huazhong University of Science and Technology, Wuhan 430074, PR China

<sup>b</sup> Hubei Key Laboratory of Material Chemistry & Service Failure, Huazhong University of Science and Technology, Wuhan 430074, PR China.

<sup>c</sup> Industrial research and development directory - Ministry of sciences and technology, Baghdad - Iraq.

### **Graphical abstract.**



### **Highlights.**

- 1) The quick precipitation (QPT) was a new route for the preparation of metal oxide nanoparticles catalyst was developed by strategy in this work.
- 2) This is the first report about formed (CuO-QPT-400) nanoparticles catalyst for glycerol carbonate production.
- 3) (CuO-QPT-400) was worked as a best and new as a metal oxide nanoparticle catalyst to produce glycerol carbonate by the carbonylation of Glycerol with Carbone Dioxide.

### **Abstract:**

Two types of metal oxide nanoparticle catalysts Lanthanum oxide (La<sub>2</sub>O<sub>3</sub>) and Copper oxide (CuO) are prepared by new method which was quick precipitation (QPT) method at calcination temperature of 400°C for 4h and used for the synthesis of glycerol carbonate from the direct reaction by the carbonylation of Glycerol with Carbone Dioxide. The quick precipitation (QPT) was a new and important route for the preparation of nanoparticles catalyst and it was developed by strategy in this work. The effects of performance of (La<sub>2</sub>O<sub>3</sub> and CuO) nanoparticle catalysts on the conversion of glycerol, yield of glycerol carbonate, selectivity of glycerol carbonate and Turnover frequency are researched. XRD, FT-IR and SEM are used for the characterization of the prepared metal oxide catalysts. It is found that the best metal oxide nanoparticles catalyst in GL carbonylation reaction is CuO prepared by quick precipitation (QPT) method at calcination temperature of 400°C for 4h. Under 150 °C, 4MPa (≈ 40 bar.), 5h, and CuO catalyst amount 37.6% (based on ratio of glycerol weight) by using 2-pyridinecarbonitrile (C<sub>6</sub>H<sub>4</sub>N<sub>2</sub>) as dehydrating agent and dimethylformamide (DMF) as solvent, the glycerol

conversion, glycerol carbonate yield and selectivity are 48.64%, 38.88%, and 79.94%, respectively, and the turnover frequency (TOF) value of the catalyst can reach  $0.2061\text{h}^{-1}$ , and the catalysts could be easily regenerated by washing with methanol and water after a reaction and then dried at  $60\text{ }^{\circ}\text{C}$  overnight after that calcination at  $400\text{ }^{\circ}\text{C}$  for 4h without loss of activity after five recycling times.

**Keywords:** *glycerol ; glycerol carbonate ; carbon dioxide ; metal oxide nanoparticle catalyst ; CuO nanoparticle catalyst ; carbonylation ;  $\text{La}_2\text{O}_3$ ; DMF.*

## 1. Introduction.

In recent years, huge amounts of glycerol (GL) are produced as a by-product of the biodiesel manufactures [1, 2]. Because of rapidly increasing production of global biodiesel in a great quantity, it becomes a research and study focus to transform GL to value-added chemicals. One of the derivatives of GL is the glycerol carbonate (GC), GC has a number of science and industrial applications such as a polar high boiling solvent, chemical intermediate, a surfactant component, carrier in batteries, lubricating oils, monomer for polymers and as components for gas separation membranes [3-5].

GC can be synthesized from GL via several routes, which can be divided into two categories: indirect and direct routes, according to different carbonyl sources. GC can be indirectly synthesized by the transesterification of GL with other organic carbonates and urea. However, carbonates such as dimethyl or diethyl carbonate would be relatively expensive chemicals leading to less commercial benefit for the transesterification of GL with them [6-8]. Meanwhile, ammonia is produced in glycerolizes of urea, which need low-pressure reaction condition to remove the ammonia gas [9-12]. Compared with the indirect route, the direct synthesis of GC by GL carbonylation with  $\text{CO}_2$  is more interesting and its atom utilization is as high as 87% [13,14]. Moreover, this reaction is regarded as a green process in which two cheap raw reactants, GL, a by-product of biodiesel production, and  $\text{CO}_2$ , a primary greenhouse gas, can be converted to a value-added chemical, Among this method, the most suitable industrial process for producing GC is the carbonylation of GL with  $\text{CO}_2$  due to the non-toxic raw material, mild operation condition, high selectivity of GC and simple purification of GC [15-17].

The first work attempt was carried out by Vieville et al. [18] using GL and  $\text{CO}_2$  gas under supercritical conditions as reactants in the presence of zeolites and basic ion-exchange resins as catalyst, when adding the co-reactant materials such as ethylene carbonate, could GC be formed. Even though the yield of GC could reach 32%, there was no evidence about the direct insertion of  $\text{CO}_2$ . Also the metal-impregnated zeolite [19] and Tin complexes [20] were reportedly for the carbonylation of glycerol with  $\text{CO}_2$ , but the conversion of glycerol was not high came to only 2.5% ( $180\text{ }^{\circ}\text{C}$ , 5 MPa, 6 h) and 5.8% ( $180\text{ }^{\circ}\text{C}$ , 10 MPa, 3h), respectively. Thermodynamic calculations showed that the low conversion of GL to GC was because of the number of equilibrium limitations [21], so dehydrate should be used to change the thermodynamic limit. 13X type of zeolite and acetonitrile were employed for this purpose with both  $\text{Cu/La}_2\text{O}_3$  [22],  $\text{Bu}_2\text{SnO}$  [7] and achieved to a good result. Despite of all these improvements, the conversion of GL is still relatively low and it is a challenge to improve and develop new effective catalytic system.

To produce GC from GL with dimethyl carbonate (DMC) by transesterification of GL process can be obtained high conversion and high yield by using a suitable catalyst such as alkali metal or carbonate or hydroxide (for example,  $\text{K}_2\text{CO}_3$ , KOH, NaOH),  $\text{Mg/Al/Zr}$  mixed oxide,  $\text{Mg/Al}$  hydrotalcite, calcium diglyceroxide, alkaline earth metal oxide (CaO) and others [23-28].

In general nanoparticle metal oxide heterogeneous catalysts are a technologically very important as acid-base and unique redox properties such as ( $\text{La}_2\text{O}_3$ ,  $\text{CeO}_2$ ,  $\text{NiO}$ ,  $\text{CuO}$  and  $\text{Co}_3\text{O}_4$  and others) [29].

Kankanit Phiwang et al. [30], reported that the Catalyst preparation  $\text{CuO}$  nanostructures catalysts by traditional Precipitation (PT) method using copper chloride ( $\text{CuCl}_2$ ) and copper nitrate ( $\text{Cu}(\text{NO}_3)_2 \cdot 3\text{H}_2\text{O}$ ). First, each precursor was dissolved in 100 ml deionized water to form 0.1 M concentration.  $\text{NaOH}$  solution (0.1 M) was slowly dropped under vigorous stirring until pH reached to 14. Black precipitates were obtained and repeatedly washed by deionized water and absolute ethanol for several times till pH reached 7. Subsequently, the washed precipitates were dried at  $80\text{ }^\circ\text{C}$  for 16 h. Finally, the precursors were calcined at ( $400\text{-}500$ )  $^\circ\text{C}$  for 4h.

Jun-Gill Kang et al. [31], They prepared of the  $\text{La}_2\text{O}_3$  Nano catalysts in a traditional Precipitation (PT) method by dissolving 10 mL of  $\text{La}(\text{III})$  nitrate hexahydrate ( $\text{La}(\text{NO}_3)_3 \cdot 6\text{H}_2\text{O}$ ) in 15mL deionized water. The ( $\text{La}(\text{NO}_3)_3 \cdot 6\text{H}_2\text{O}$ ) solution and of deionized water were then mixed in a Teflon bottle, and (0.5 – 2.0) mL of an ammonia solution was then added slowly drop wise under vigorous stirring to obtain a white precipitate keeping the pH value ( $10 \pm 1$ ). The bottle was capped tightly and kept in an oven ( $120\text{ }^\circ\text{C}$ ) for 12h. After the reaction, the precipitates were washed sequentially with deionized water and ethanol, the final precipitates were collected and then dried in an air convection oven ( $80\text{ }^\circ\text{C}$ ) for 24h. The as prepared powder samples were calcined to obtain  $\text{La}_2\text{O}_3$  at  $400$ ,  $700\text{ }^\circ\text{C}$  (or  $900\text{ }^\circ\text{C}$ ) for 4h.

Metal oxide nanoparticle is an important kind of catalysts with a high surface area and a high catalyst activity. In more and more reactions, metal oxide nanoparticle works as a catalyst showing very good performance [32-34]. For instance, Paulose et al. prepared nanoparticles copper oxide ( $\text{CuO}$ ) dispersed on alumina by sol-gel method and found the catalyst shows high catalytic activity for the thermal decomposition of ammonium perchlorate [34]. Shokrani et al. also synthesized  $\text{CuO}$ -based as nanoparticles catalyst by urea-nitrates combustion method and found that the nanocatalyst has a well practicability for hydrogen production via steam reforming of methanol [35].

In present work, we employed two type of metal oxide Nanoparticle ( $\text{La}_2\text{O}_3$  and  $\text{CuO}$ ) as the catalyst for the synthesis of GC from GL and  $\text{CO}_2$  in the presence of (2-pyridinecarbonitrile) which was used as a dehydration agent to pull water from the middle of the chemical reaction as side product and shift the chemical equilibrium to the GC production side and solvent of  $\text{CO}_2$  (Dimethylformamide (DMF)). The important objective of this work was to select the best one of two type of metal oxide Nanoparticle ( $\text{La}_2\text{O}_3$  and  $\text{CuO}$ ), and develop a new effective catalytic system (carbonylation system) to increase the reaction rate and selectivity of the carbonylation of GL. The quick precipitation (QPT) was a new route for the preparation of Nanoparticles metal oxide catalyst was developed by strategy in this research. The stability and activity of the suitable catalysts were studied in detail. From our knowledge, this is the first work of the application of prepared (Nano particles metal oxide)-based catalyst for using in the carbonylation of GL reaction for GC production.

## 2. Experimental Section.

### 2.1. Chemicals.

Lanthanum nitrate hex hydrate [ $\text{La}(\text{NO}_3)_3 \cdot 6\text{H}_2\text{O}$ ]  $\geq 90\%$  purity, Copper(II) nitrate trihydrate [ $\text{Cu}(\text{NO}_3)_2 \cdot 3\text{H}_2\text{O}$ ] 99% purity, (25 wt.%) ammonia solution, Glycerol GL 99% purity and N.N Dimethylformamide(DMF) ( $\text{C}_3\text{H}_7\text{NO}$ ) 99% purity were bought from Sinopharm Chemical Reagent Co., Ltd., Beijing-China. 2-pyridinecarbonitrile were purchased from Aladdin Industrial Corporation Co., Shanghai-China.

Carbon dioxide (CO<sub>2</sub>) 99.9% purity was supplied by Sichuan Tianyi Science & Technology Co., Ltd., Sichuan-China. All these chemicals were used without further purification.

## **2.2. Catalyst preparation method.**

The quick precipitation (QPT) method was a new route for the preparation of metal oxide nanoparticles catalyst and it was developed by strategy in this work, the amounts of materials depended on the stoichiometric of materials to prepared the metal oxide nanoparticles catalysts:

### **(CuO) nanoparticles catalysts preparation:**

300ml of Copper(II) nitrate trihydrate [(Cu(NO<sub>3</sub>)<sub>2</sub>·3H<sub>2</sub>O) 0.21mol/L solution was put into a 500ml Boiling Flask and heated to 80°C with constant stirring (500 rpm) by using oil bath. The color of the mixture was bright (saturated case) about 3h. About 100 mL of 25% NH<sub>3</sub> (1mol/L) solution (1M) was rapidly added into the mixture, and a Nanoparticle suspension was formed, the suspension was kept at 60 °C for 1 h and keeping the pH value (10 ± 1). An amount of black precipitate was filtered and washed with deionized water for five times, and after that dried at 60°C in vacuum dryer for 2h, and then grinded to (100) mesh scale, followed by calcination at 400°C for 4 h in air. The obtained product was denoted as (CuO-PT-400). The sample was calcined at different temperatures were named as [CuO- PT- T (T means the calcination temperature)].

### **(La<sub>2</sub>O<sub>3</sub>) nanoparticles catalysts preparation:**

300ml of Lanthanum nitrate hex hydrate [La(NO<sub>3</sub>)<sub>3</sub>·6H<sub>2</sub>O] 0.05mol/L solution was put into a 500ml Boiling Flask and heated to 80°C with constant stirring (500 rpm) by using oil bath. The color of the mixture was bright (saturated case) about 3h. About 100 mL of 25% NH<sub>3</sub> (1mol/L) solution (1M) was rapidly added into the mixture, and a Nanoparticle suspension was formed, the suspension was kept at 60 °C for 1 h and keeping the pH value (10 ± 1). An amount of black precipitate was filtered and washed with deionized water for five times, and after that dried at 60°C in vacuum dryer for 2h, and then grinded to (100) mesh scale, followed by calcination at 400°C for 4 h in air. The obtained product was denoted as (La<sub>2</sub>O<sub>3</sub>-PT-400). The sample was calcined at different temperatures were named as [La<sub>2</sub>O<sub>3</sub>- PT- T (T means the calcination temperature)].

## **2.3. Catalyst characterization**

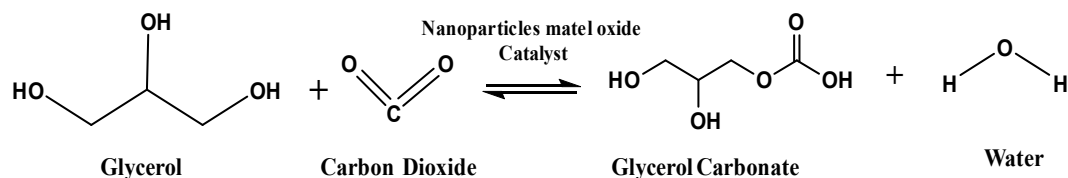
X-ray diffraction (XRD) patterns of the catalysts were measured on a X'Pert PRO using Cu K $\alpha$  radiation at 30 kV and 15 mA, over a 2 $\theta$  range of 5-90° with a step size of 0.0167° at a scanning speed of 8min<sup>-1</sup>.

Bruker VERTEX 70 FT-IR spectrometers was used to obtained the FT-IR spectra of samples using KBr pellet technique, with 2 cm<sup>-1</sup> resolution over the wavenumber range (4000–400) cm<sup>-1</sup>.

The morphology of the particles was observed by use of a scanning electron microscope (SEM, TESCAN VEGA3) with 20.0 kV of an accelerating voltage.

## **2.4. Reaction procedure.**

Glycerol carbonate (GC) was obtained from the carbonylation of glycerol (GL) and CO<sub>2</sub> over nanoparticles catalysts. As shown in scheme 1.



**Scheme1.** Carboxylation of glycerol and CO<sub>2</sub> over nanoparticles metal oxide catalysts.

The tests of the catalytic activities of the nanoparticles metal oxide catalysts were carried out in a stainless-steel autoclave reactor system with an inner volume of 200ml and it has thermostat with an electric heating jacket, pressure gauge and agitator, the autoclave reactor was one of the most important chemical engineering equipment and its operation is not easy, it requires attention and caution when operating, because it works under conditions of high temperature and high pressure. After ascertaining the validity of the autoclave system (fig.1.), the typical procedure is as follows: 40mmol glycerol (GL), 37mmol% Cat./GL, 16 g of Dimethylformamide (DMF) and 6 g of 2-pyridinecarbonitrate, were added into the autoclave together, and then the reactor was sealed, purged with N<sub>2</sub> or CO<sub>2</sub> for 3 times and then pressurized with CO<sub>2</sub> to 4 MPa. Subsequently, the autoclave was heated to the reaction temperature (150 °C) and maintained for certain reaction time (5h) under vigorous stirring. After reaction, the reactor was cooled to room temperature and depressurized, the product mixture was taken out from the autoclave reactor to centrifugal filtration 5000 rpm for 6 min to separate the solid catalyst and liquid products, after that take all liquid product to analyzing.

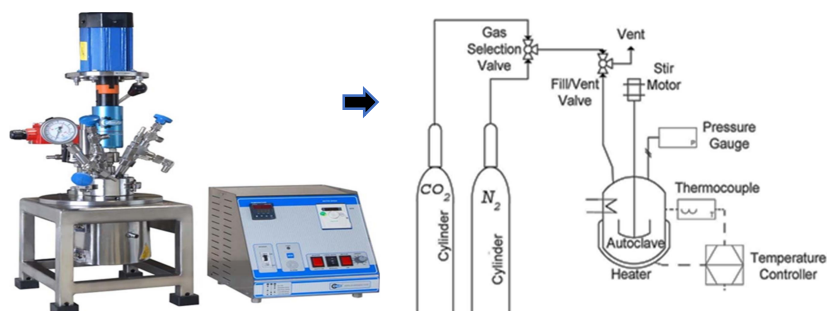


**Fig. 1.** Autoclave reactor system.

## 2.5. Liquid product analysis.

All the components in liquid product were analyzed by the gas chromatograph (Fuli 9790-II) equipped with a flame ionization detector (FID) and a capillary column DM-FFAP (30 m long, 0.25 mm id). The internal standard method was used. Hydrogen (H<sub>2</sub>) nitrogen (N<sub>2</sub>) (99.999% pure) and air (20.8% O<sub>2</sub>, 79.2% N<sub>2</sub>), were supplied by (Sichuan Tianyi Science & Technology Co., Ltd., Sichuan, China), air and N<sub>2</sub> were used as the carrier gas with a flow rate of 30 mL/min at 0.4 MPa and H<sub>2</sub> at 0.25MPa. The temperatures of the injector and the detector were 250 °C and 270 °C, respectively. The temperature of the column was programmed to have a 2min initial hold at 70 °C, a 15 °C/min ramp from 70 °C to 250 °C and a 15 min hold at 250 °C. A good peak separation was achieved under these conditions for all components. n- Butanol was used as the internal standard to determine Methanol, while tetra ethylene glycol was used as the internal standard to determine GL and GC. Added about 1g methanol to liquid product sample for diluting before injecting into gas chromatograph (Fuli

9790-II), the mass of all sample was (mass of samples + mass of ethanol) to determining the mass of GL and GC output with product.

The conversion of GL,  $X_{GL}$ , and the yield of GC,  $Y_{GC}$ , and selectivity of GC,  $S_{GC}$  and the Turnover frequency (TOF) were calculated according to the following equations:

$$\text{Conversion}(X_{GL}) = \frac{n_{GL.in} - n_{GL.out}}{n_{GL.in}} \times 100 \quad (1)$$

$$\text{yield}(Y_{GC}) = \frac{n_{GC.out}}{n_{GL.in}} \times 100 \quad (2)$$

$$\text{Selectivity}(S_{GC}) = \frac{Y_{GC}}{X_{GL}} \times 100 \quad (3)$$

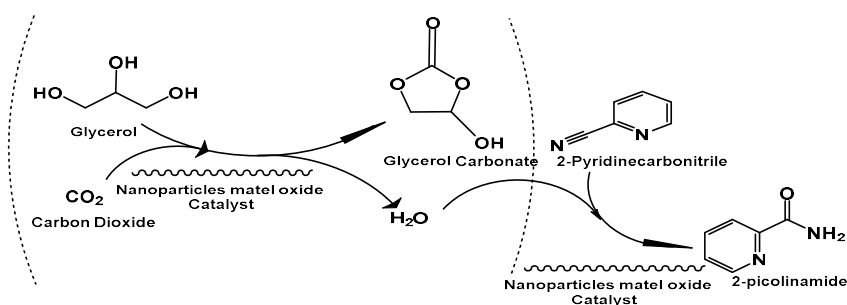
$$\text{TOF (Turnover frequency)} = \frac{n_{GC.out}}{n_{cat.} \times \text{time (h)}} \quad (4)$$

Where  $n_{GL.in}$  the number of initial moles of GL,  $n_{GL.out}$  is the number of moles of GL output (unreacted),  $n_{GC.out}$  is the number of moles of GC product and  $n_{cat.}$  is the number of moles of catalyst.

A catalyst's turnover frequency number, or turnover number per time unit, characterizes its level of activity. So, the TOF is the total number of moles transformed into the desired product by one mole of active site per hour. The large one of the TOF that means more active catalyst.

### 3. Result and discussion.

The synthesis of GC from GL and  $CO_2$  by carbonylation reaction over metal oxide nanoparticles catalyst in the presence of (2-pyridinecarbonitrile), which was used as a dehydration agent to pull water from the middle of the chemical reaction as byproduct to produced 2-picolinamide ( $C_6H_6N_2O$ ) and shift the chemical equilibrium to the GC production side and solvent of  $CO_2$  Dimethylformamide (DMF). As shown in mechanism of carboxylation reaction in scheme 2. The conditions of reaction were (150 °C temperature, 5h time, and 4MPa initial pressure of  $CO_2$  and 500 rpm of mixing. The gas chromatogram of the reaction mixture is given in Fig. 2 it can be found a good peak separation is achieved for all components.



**Scheme2.** Mechanism of carboxylation of glycerol by  $CO_2$  and dehydration over nanoparticles metal oxide catalysts as the coupling reaction.

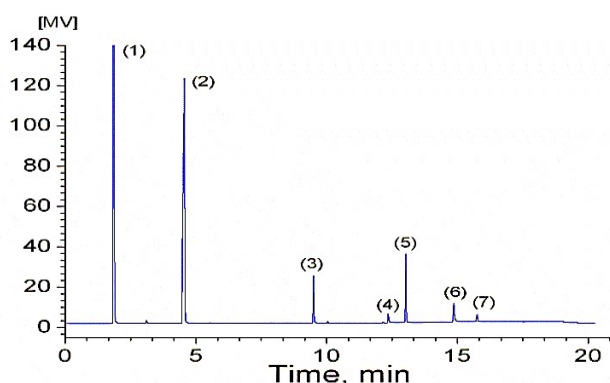


**Fig.2** The gas chromatogram of the reaction mixture ((1) methanol, (2) DMF, (3) 2-pyridincarboxonitrile, (4) GL, (5) 2-picolinamide, (6) tetra ethylene glycol, (7) GC).

### 3.1. Effect of type of nanoparticles metal oxide catalyst.

Two types of metal oxide nanoparticle catalysts (CuO-QPT-400) and (La<sub>2</sub>O<sub>3</sub>-QPT-400) were used in carbonylation of GL with CO<sub>2</sub> to produce GC and their catalytic performances and presented in Table 1. Among two catalysts, the (CuO-QPT-400) nanoparticle has the highest catalytic performance; in contrast, La<sub>2</sub>O<sub>3</sub>-QPT-400 shows the lowest activity for the reaction of GL with CO<sub>2</sub>. Over (CuO-QPT-400) catalyst, the GL conversion ( $X_{GL}$ ), GD yield ( $Y_{GC}$ ), and GD selectivity ( $S_{GC}$ ) and the Turnover frequency (TOF) were determined by equations (1, 2, 3, 4) and we could reach 48.64%, 38.88%, and 79.94%, respectively, while the TOF value reach 0.2061 h<sup>-1</sup> as shown in table1. The results mean (CuO-QPT-400) nanoparticle is a good catalyst for carbonylation of GL with CO<sub>2</sub>.

**Table. 1.** The catalytic performances of the metal oxide nanoparticle catalysts in the carbonylation of GL with CO<sub>2</sub> to produce GC <sup>a</sup>

| Cat.                                    | $X_{GL}/\%$ | $Y_{GC}/\%$ | $S_{GC}/\%$ | TOF/h <sup>-1</sup> <sup>b</sup> |
|-----------------------------------------|-------------|-------------|-------------|----------------------------------|
| CuO-QPT-400                             | 48.64       | 38.88       | 79.94       | 0.2061                           |
| La <sub>2</sub> O <sub>3</sub> -QPT-400 | 22.62       | 12.14       | 53.65       | 0.0687                           |

<sup>a</sup> Reaction condition: 40 mmol GL, 37.7mmol % Cat./GL, 5 g of 2-pyridinecarboxonitrile, 15g DMF, 150 °C, 4 MPa CO<sub>2</sub> and 5h.

<sup>b</sup> TOF: Turnover frequency (h<sup>-1</sup>).

The catalytic performances were presented in Table1. Show high conversion of GL., high yield of GC, high selectivity of GC. And high TOF with (CuO-QPT-400) Nano catalyst when compared with (La<sub>2</sub>O<sub>3</sub>-QPT-400) and ranked as:

$$(CuO-QPT-400) > (La_2O_3-QPT-400)$$

And the (CuO-QPT-400) was more activity than (La<sub>2</sub>O<sub>3</sub>-QPT-400) catalysts because it has more TOF.

### 3.2 Catalyst characterization.

#### 3.2.1 XRD.

Fig.3 shows the XRD patterns of (CuO and La<sub>2</sub>O<sub>3</sub>) nanoparticles catalysts calcined at temperature (400 °C). The samples present a typical band of CuO phase with monoclinic crystal system Ref. Code(00-048-1548) (at  $2\theta = 32.5, 35.5, 38.8, 46.2, 48.8, 51.4, 53.5, 58.3, 61.5, 66.3, 68.13, 72.5, 75.1, 80.1, 82.5, 83.1, 83.6$  and see PDF-2....e2004-163835) also a typical band of La<sub>2</sub>O<sub>3</sub> phase with monoclinic crystal system Ref. Code(00-040-1281)

(at  $2\theta = 25.329, 27.725, 28.936, 37.902, 44.635, 49.795, 52.015, 54.073, 59.597$  and see PDF-2....e2004-163835 ) In Fig. 3, it is also found that for CuO-QPT-400 sample, indicating the gradual bulk sintering and growth of crystallite size of CuO-QPT-400. All the catalysts show clear and sharp peaks of CuO-QPT-400 more than  $\text{La}_2\text{O}_3$ -QPT-400 and the diffraction intensity of crystal face (111) is stronger than of crystal face (110), in contrast, for  $\text{La}_2\text{O}_3$ -QPT-400, the diffraction intensity of crystal face (110) is stronger than of crystal face (111). The width of the diffraction lines is produced using the smaller grains. The diffraction peaks of nanoparticles  $\text{La}_2\text{O}_3$ -QPT-400 were broader, which indicates the presence of small particles in the former catalysts. It means that the effectiveness of the  $\text{La}_2\text{O}_3$ -QPT-400 was a little and less than CuO-QPT-400, which is accordant with the order of the catalytic activity for these catalysts (Table 1, except with CuO-QPT-400), meaning that the crystal face (111) for CuO-QPT-400 nanoparticles catalyst may be have more active site for the carbonylation of GL with  $\text{CO}_2$ .

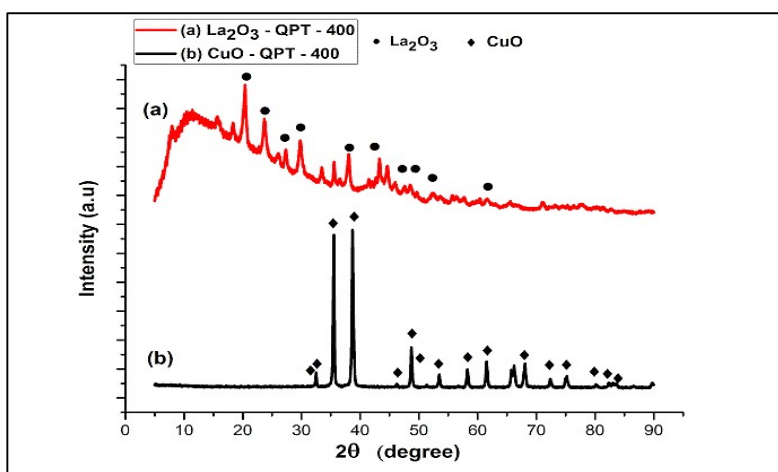


**Fig.3** XRD patterns of the nanoparticle catalysts: (a)  $\text{La}_2\text{O}_3$ -QPT-400, (b) CuO-QPT-400.

### 3.2.2 FT-IR.

The FT-IR analysis results are depicted in Fig. 5 for CuO-QPT-400 nanoparticles catalyst with different calcination temperature. For all samples the peak positions are approximately similar indicating they have the same surface functional groups. The peaks appearing at  $517$  and  $598\text{ cm}^{-1}$  are attributed to (Cu-O) stretching modes.

The FT-IR analysis results are depicted in Fig.4 for CuO-QPT-400 nanoparticles with  $(400\text{ }^\circ\text{C})$  calcination temperature. For all samples the peak positions are approximately similar indicating they have the same surface functional groups. The peaks appearing at  $517$  and  $598\text{ cm}^{-1}$  are attributed to (Cu-O) and ( $\text{La}_2\text{-O}_3$ ) stretching modes. The peaks at  $1384\text{ cm}^{-1}$  may be assigned to (O-H) bending vibrations combined with copper atoms. Furthermore, peaks at around  $3460\text{ cm}^{-1}$  show the existence of the hydroxide group. The FT-IR result suggests the formation of CuO compound and is consistent with the XRD.



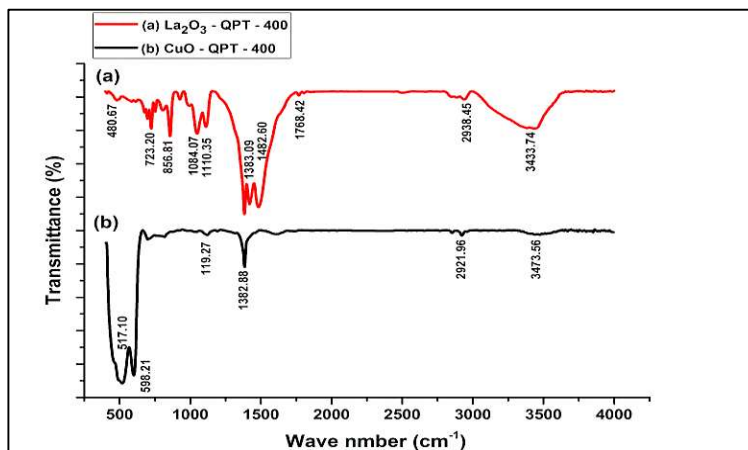


**Fig. 4.** FT-IR spectra of nanoparticles catalysts: (a) La<sub>2</sub>O<sub>3</sub>-QPT-400, (b) CuO-QPT-400.

### 3.2.3 SEM.

The Morphology of (La<sub>2</sub>O<sub>3</sub>-QPT-400) and (CuO-QPT-400) nanoparticles catalyst prepared with quick precipitation method (QPT) was examined by scanning electron microscope (SEM).

The SEM images of the catalysts are shown in Fig.5 (a, b). It can be seen that all samples present aggregates of variable morphology and size. The nanoparticles for (CuO-QPT-400) catalyst (Fig.5a) was a best one because of particles size distribution was homogenous (160nm – 320nm) and high surface area and good dispersion and It shows that higher tendency of agglomerations but the nanoparticles for (La<sub>2</sub>O<sub>3</sub>-QPT-400) catalyst (Fig. 8b) are obviously the particles size distribution of (1.163μm – 921.5nm) that means this particles size distribution not homogenous and a little surface area and the (La<sub>2</sub>O<sub>3</sub>-QPT-400) is formed through the accumulation of small particles, it was consisted of loose and tiny floc and tightly gathered with a large lump and a little stripe structure. It means, among these samples, CuO-PT-400 has the particle with the smallest size and the most uniform shape, resulting in the best catalytic activity. The SEM result suggests the formation of CuO-PT-400 nanoparticles catalyst and is consistent with the XRD, which is accordant with the order of the catalytic activity for these catalysts (Table 1, except with CuO-QPT-400).

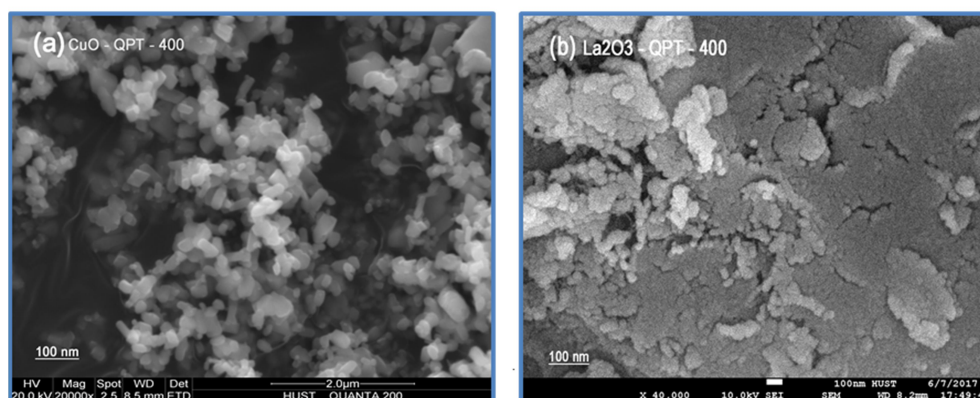


**Fig. 5.** SEM a scanning electron microscope images of the fresh nanoparticles catalysts (a) CuO-QPT-400, (b) La<sub>2</sub>O<sub>3</sub>-QPT-400.

### 3.3 Stability of the CuO-QPT-400 nanoparticle catalyst.

When choose the best one which is CuO-QPT-400 nanoparticles catalyst is very important to complete all the functions of using the catalyst and one of these functions is recyclability of catalyst several times at least five times, the used catalysts were recovered. The stability of CuO-QPT-400 was also researched and the result is shown in Fig. 6.

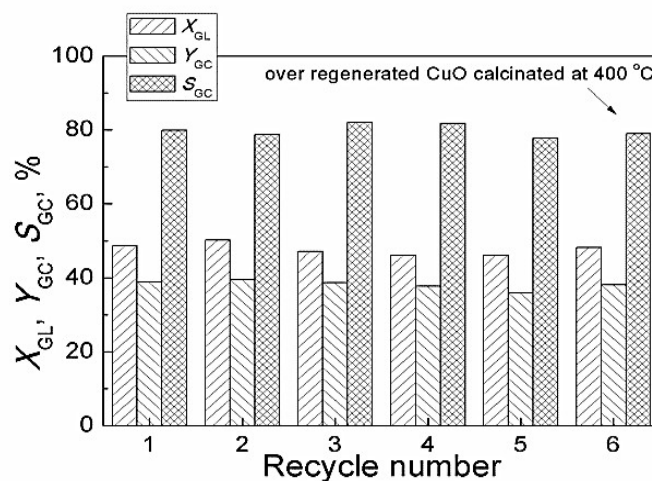


**Fig. 6.** The stability of CuO-QPT-400 nanoparticle catalyst on the reaction of GL with CO<sub>2</sub>(Reaction condition: 40 mmol GL, 37.7mmol % Cat./GL, 5 g of 2-pyridinecarbonitrates, 15g DMF, 150 °C, 4 MPa CO<sub>2</sub>, 5 h).

It is found that at the fourth recycling, the activity of CuO-QPT-400 hardly decreases and the GL conversion and GC yield can also reach 46.09% and 37.71%, respectively. At the fifth recycling, the GL conversion and GC yield reach 46.10% and 35.86%, respectively, indicating that the activity of CuO-QPT-400 slightly decreases. In order to ascertain the reason of the decrease of the catalytic activity for the CuO-QPT-400 catalyst, the recovered CuO-QPT-400 in the fifth recycling was also characterized by XRD and FT-IR. Fig. 7.(a) XRD shows that the crystalline structure of recovered CuO-QPT-400 is changed, and it has a strong cubic Cu phase ( $2\theta = 43.5^\circ, 50.65^\circ$ , see PDF 00-001-1242). Fig. 8.(a) shows that in the FT-IR spectra of recovered CuO-QPT-400, the characteristic peaks attributed to Cu-O stretching mode (at 517 and 598  $\text{cm}^{-1}$ ) are vanished. These results imply that generation of Cu phase is responsible for the deactivation of the CuO-QPT-400 catalyst. Interestingly, when the recovered CuO-QPT-400 is calcined at 400 °C, its main phase can be converted back into the monoclinic CuO again (Fig. 7 (b) and Fig. 8 (b)). Meanwhile, the regenerated catalyst CuO-QPT-400 was used to the reaction of GL and CO<sub>2</sub> and also can produce GL conversion of 48.25% and GC yield of 38.10% (Fig. 10). It indicates that the recovered catalyst CuO-QPT-400 can be easily regenerated by calcining at 400 °C. Furthermore, the Cu concentration in the reaction mixture in the first run was also measured by inductively coupled plasma-mass spectrometry (ICP-MS) and the result only was 45.12  $\mu\text{g/L}$ , indicating that the leaching of CuO almost can be neglected.

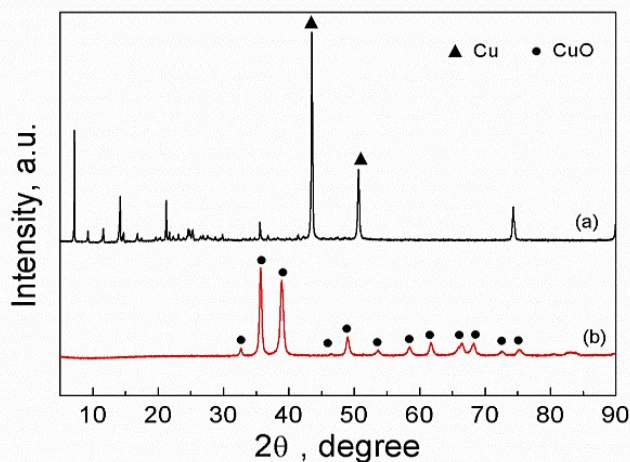


**Fig. 7.** XRD patterns of the CuO nanoparticle catalysts: (a) the recovered CuO-QPT-400 catalyst after the fifth recycling; (b) the recovered CuO-QPT-400 catalyst regeneration by again calcination at 400 °C.

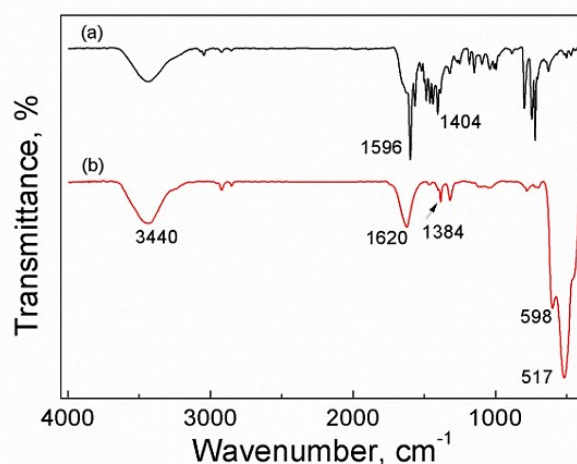
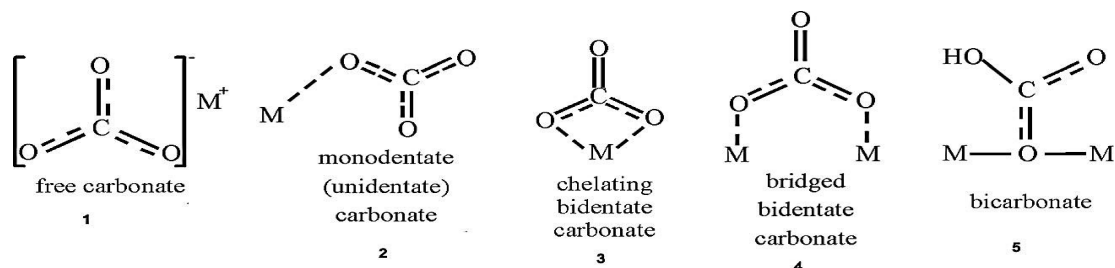


**Fig.8.** FT-IR spectra of CuO nanoparticles catalysts: (a) the recovered CuO-QPT-400 catalyst after the fifth recycling; (b) the recovered CuO-QPT-400 catalyst regeneration by again calcination at 400 °C.

#### **4. The possible mechanisms of glycerol carbonate synthesis at carboxylation reaction over (CuO-QPT-400) nanoparticles catalyst.**

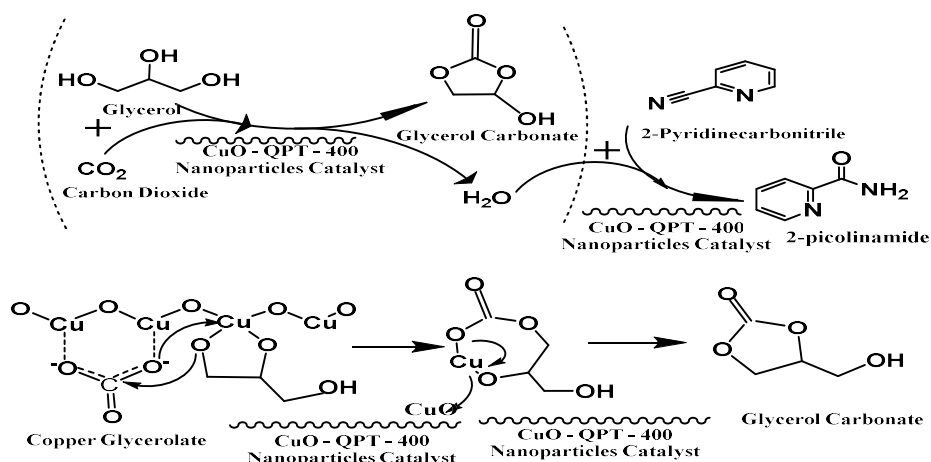
In order to understand the reaction mechanism, in chemical engineering this reaction was heterogeneous reaction because the reactants at difference phase, glycerol (GL) is liquid, CO<sub>2</sub> is gas and (CuO – QPT – 400) nanoparticles catalyst was solid. Poor conversion and mass-balance of glycerol were gained when no solvent was applied. To improving the reaction rates should be dissolve CO<sub>2</sub> in middle of the reaction until it reaches the surface of the catalyst. Supercritical carbon dioxide (ScCO<sub>2</sub>) at (7.5 MPa, 150 °C) is considered to be a highly attractive modern solvent compared to traditional organic solvents, the solvent employed in this study, DMF gave the maximum yield of glycerol carbonate, indicating that the solvent effect in our CuO/2-cyanopyridine system was one of the important factors responsible for the much better catalytic performance. Solvents usually show some effects on reaction rates, chemical equilibrium as well as reaction mechanisms in

organic reactions. It had been proposed that for GL reacting with CO<sub>2</sub> to form GC over CuO surface in the presence of 2-pyridinecarbonitrile and DMF, nucleophile attack of the other OH group to the carbonyl carbon in carbonate species, which led to the production of cyclic carbonate and water, was one of the important steps in the proposed reaction mechanism. Since the nucleophilicity of the reactants was affected in dipolar aprotic solvent [36], the step mentioned above could be enhanced in DMF. On the other hand, the solubility of CO<sub>2</sub> in the solvents might also be an important factor besides the polarity and aprotic properties of the solvents. The basic nature of DMF may favor the dissolving and adsorption of CO<sub>2</sub>. In fact, the solubility of CO<sub>2</sub> in DMF is 31.1 mol% at 40°C and 4.5 MPa [37]. Therefore, high solubility of CO<sub>2</sub> in DMF might be favorable to increase the concentration of CO<sub>2</sub> on the surface of the catalysts, consequently benefiting to the reaction. The CO<sub>2</sub> adsorption modes identified in previous work are shown in **Scheme 3**. [38-40]. The formation of different species might stem from different basic sites: e.g. (1). Free carbonate (FC) (2). Monodentate (unidentate) carbonate (MC), adsorbed on oxygen ions with the lowest coordination number, can be attributed to strongly basic sites, (3). Chelating bidentate carbonate (CBC) and (4). Bridged bidentate carbonate (BBC) adsorbed on (M<sup>+</sup> – O<sub>2</sub><sup>-</sup>) pairs can be assigned to moderately basic sites Moreover, the weakly basic sites may be associated with the surface hydroxyl groups (OH<sup>-</sup>) over which the CO<sub>2</sub> adsorption species is present in the form of (5). Bicarbonate [39].



**Scheme 3.** Types of species of CO<sub>2</sub> adsorption.

The cyclic carbonate was formed through the insertion of activated CO<sub>2</sub> to metal alkoxides followed by intermolecular nucleophile attack of alkoxy groups to carbonyl carbon atoms. In our experiment, the bridged bidentate carbonate was the main adsorption mode at 150 °C (reaction temperature) on the catalysts. Therefore, the activated CO<sub>2</sub> may be in the form of a bridged bidentate carbonate that inserts into the copper glycerolate to form a cyclic metal carbonate (as in **Scheme 4**) followed by intermolecular rearrangement to produce glycerol carbonate. The copper glycerolate reaction with CO<sub>2</sub> and theoretical calculations indicate that the proposed reaction mechanism is reasonable, that the A species produced by the insertion of activated CO<sub>2</sub> to copper glycerolate is stable and that the process happens spontaneously. The process of glycerol carbonate formation by the intermolecular rearrangement of the A species is the rate-determining step. Glycerol carbonate was obtained from the carbonylation of glycerol and CO<sub>2</sub> over CuO Nano catalysts with the hydrolysis of 2-pyridinecarbonitrile as the coupling reaction. As shown in Scheme 4, in the CuO/2-pyridinecarbonitrile system, glycerol reacts with CO<sub>2</sub> over CuO catalyst surface to produce glycerol carbonate and H<sub>2</sub>O, while the formed H<sub>2</sub>O reacts with 2-pyridinecarbonitrile (2-cyanopyridine) to produce (2 – picolinamide) and removed H<sub>2</sub>O from the reaction system to pull water from the middle of the chemical reaction as side product and shift the chemical equilibrium to the GC production side and the chemical reaction bath doesn't return back to reverse direction to produce GL [7, 41, and 42].



**Scheme 4.** The reaction roadmap and the mechanism of insertion of activated CO<sub>2</sub> to copper glycerolate to form glycerol carbonate (Reaction condition: 40mmol glycerol, 37.7 mmol % Cat./GL, 5 g of 2-pyridinecarbonitrile, 15 g of DMF, 150 °C and 4 MPa CO<sub>2</sub> for 5h).

## 5. Conclusion.

CuO nanoparticle was synthesized by new method it is quick precipitation (QPT). It showed the best one and excellent catalytic performance among two type of nanoparticles metal oxide catalyst (La<sub>2</sub>O<sub>3</sub> and CuO) in the carbonylation of glycerol and CO<sub>2</sub> with 2-cyanopyridine as a dehydrating agent. The active site of CuO catalyst may be crystal face (111). The incredibly yield of glycerol carbonate GC (can reach about 40%) had strong relevance with the efficient dehydration agent of 2-pyridinecarbonitrile (2-cyanopyridine) and solvent effect of DMF and (400) °C was a good calcination temperature. The proper reaction conditions were (5.0- 7.0) g 2-pyridinecarbonitrile (3 times of stoichiometric value), 150 °C, 4 MPa and 5 h. The active site of the CuO catalyst is all CuO. The catalyst not only has higher surface area, but also higher mechanical strength, and is suitable for the industrial reactor. The stability research for CuO nanoparticle shows that the catalyst can be reused five times with little loss of activity and can be easily regenerated by calcination at 400 °C. In our future work, the suitable support for this catalyst and mixed this catalyst with another suitable nanoparticles metal oxide catalyst will be investigated and reported in due course.

## Acknowledgements.

We acknowledge the financial support by the National Natural Science Foundation of China (21106050), the Specialized Research Foundation for the Doctoral Program of Ministry of Education of China (20100142120066), and the Fundamental Research Funds for the Central Universities of China (2011QN117). XRD and SEM analysis was performed in the Analytical and Testing Center, and FT-IR analysis was performed in the Experimental Teaching Center of chemistry and Chemical Engineering, School of Chemistry and Chemical Engineering, Huazhong University of Science and Technology. Also we acknowledge the financial support by Industrial research and development directory - Ministry of sciences and technology, Baghdad - Iraq.

## References.

- [1]. M. Aresta, A. Dibenedetto, F. Nocito, C. Pastore, A study on the carboxylation of glycerol to glycerol carbonate with carbon dioxide: the role of the catalyst, solvent and reaction conditions, *J. Mol. Catal. A: Chem.* 257 (2006) 149–153.
- [2]. A. Behr, J. Eilting, K. Irawadi, J. Leschinski, F. Lindner, “Improved utilization of renewable resources: New important derivatives of glycerol” *Green Chem.* 10 (2008) 13-30.
- [3]. S.Y. Huang, F.L. Wang, W. Wei, Y.H. Sun, A study on synthesis of glycerol carbonate from carbon dioxide and glycerol over base catalysts, *Mod. Chem. Ind.* 28 (2008) 35–37(in Chinese language).
- [4]. J.L. Hu, J.J. Li, Y.L. Gu, Z.H. Guan, W.L. Mo, Y.M. Ni, T. Li, G.X. Li, Oxidative carbonylation of glycerol to glycerol carbonate catalyzed by PdCl<sub>2</sub>(phen)/KI, *Appl. Catal. A: Gen.* 386 (2010) 188–193.
- [5]. D.P. Abraham, Electrolytes for lithium and lithium-ion batteries. U.S. Patent Appl. 2011/0117445A1 (2011).
- [6]. M.G. Alvarez, A.M. Frey, J.H. Bitter, A.M. Segarra, K.P. de Jong, F. Medina, On the role of the activation procedure of supported hydrotalcites for base catalyzed reactions: Glycerol to glycerol carbonate and self-condensation of acetone, *Appl. Catal. B-Environ.* 134-135 (2013) 231-237.
- [7]. M.G. Alvarez, A.M. Segarra, S. Contreras, J.E. Sueiras, F. Medina, F. Figueras, Enhanced use of renewable resources: Transesterification of glycerol catalyzed by hydrotalcite-like compounds, *Chem. Eng. J.* 161 (2010) 340-345.
- [8]. F. Rubio-Marcos, V. Calvino-Casilda, M.A. Banares, J.F. Fernandez, Novel hierarchical Co<sub>3</sub>O<sub>4</sub>/ZnO mixtures by dry nanodispersion and their catalytic application in the carbonylation of glycerol, *J. Catal.* 275 (2010) 288-293.
- [9]. M. Aresta, A. Dibenedetto, F. Nocito, C. Ferragina, and Valorization of bio-glycerol: New catalytic materials for the synthesis of glycerol carbonate via glycerolysis of urea, *J. Catal.* 268 (2009) 106-114.
- [10]. M.J. Climent, A. Corma, P.D. Frutos, S. Iborra, M. Noy, A. Velty, P. Concepcion, Chemicals from biomass: Synthesis of glycerol carbonate by transesterification and carbonylation with urea with hydrotalcite catalysts. The role of acid-base pairs, *J. Catal.* 269 (2010) 140-149.
- [11]. M.H.A. Rahim, Q. He, J.A. Lopez-Sanchez, C. Hammond, N. Dimitratos, M. Sankar, A.F. Carley, C.J. Kiely, D.W. Knight, G.J. Hutchings, Gold, palladium and gold-palladium supported nanoparticles for the synthesis of glycerol carbonate from glycerol and urea, *Catal. Sci. Technol.* 2 (2012) 1914-1924.
- [12]. Y.K. Endah, M.S. Kim, J. Choi, J. Jae, S.D. Lee, H. Lee, Consecutive carbonylation and decarboxylation of glycerol with urea for the synthesis of glycidol via glycerol carbonate, *Catal. Today* 293-294 (2017) 136-141.
- [13]. H.G. Li, C.L. Xin, X. Jiao, N. Zhao, F.K. Xiao, L. Li, W. Wei, Y.H. Sun, Direct carbonylation of glycerol with CO<sub>2</sub> to glycerol carbonate over Zn/Al/La/X(X=F, Cl, Br) catalysts: The influence of the interlayer anion, *J. Mol. Catal. A-Chem.* 402 (2015) 71-78.
- [14]. M. Aresta, A. Dibenedetto, F. Nocito, C. Pastore, A study on the carboxylation of glycerol to glycerol carbonate with carbon dioxide: The role of the catalyst, solvent and reaction conditions, *J. Mol. Catal. A-Chem.* 257 (2006) 149-153.
- [15]. M.O. Sonnati, S. Amigoni, E. de Givenchy, T. Darmanin, O. Choulet, F. Guittard “Glycerol carbonate as a versatile building block for tomorrow: synthesis, reactivity, properties and applications”, *Green Chem.* 15 (2013) 283-306.

- [16]. J. George, Y. Patel, S.M. Pillai, P. Munshi, J., "Methanol Assisted Selective Formation of 1,2-Glycerol Carbonate from Glycerol and Carbon Dioxide Using  $\text{Bu}_2\text{SnO}$  as a Catalyst," *Mol. Catal. A-Chem.* 304 (2009) 1-7.
- [17]. T. Sakakura, J.C. Choi, H. Yasuda, "C–H carboxylation of heteroarenes with ambient  $\text{CO}_2$ ", *Chem. Rev.* 107 (2007) 2365-2387.
- [18]. C. Vieville, J.W. Yoo, S. Pelet, Z. Mouloungui, "Synthesis of glycerol carbonate by direct carbonation of glycerol in supercritical  $\text{CO}_2$  in the presence of zeolites and ion exchange resins" *Catal. Lett.* 56 (1998) 245-247.
- [19]. M. Aresta, A. Dibenedetto, C. Nocito, F. Pastore, "A study on the carboxylation of glycerol to glycerol carbonate with carbon dioxide: the role of the catalyst, solvent and reaction conditions", *J. Mol. Catal. A-Chem.* 257(2006) 149–153.
- [20]. Leonardo P. Ozorioa, Rafael Pianzolib, Luciana da Cruz Machadoa, Jussara L. Mirandab, Cássia C. Turcib, Antônio C.O. Guerrab, E. Falabella Souza-Aguiara, c, Claudio J.A. Mota, "Metal-impregnated zeolite Y as efficient catalyst for the direct carbonation of glycerol with  $\text{CO}_2$ ", *Appl. Catalyt., A-Gen.* Volume 504, 5 September 2015, Pages 187–191.
- [21]. J.B. Li, T. Wang, "Chemical equilibrium of glycerol carbonate synthesis from glycerol", *J. Chem. Thermodyn.* 43 (2011) 731–736.
- [22]. J. Zhang, D. He, "Surface properties of  $\text{Cu/La}_2\text{O}_3$  and its catalytic performance in the synthesis of glycerol carbonate and monoacetin from glycerol and carbon dioxide", *J. Colloid Interface Sci.* 419 (2014) 31–38.
- [23]. S.C. Kim, Y.H. Kim, H. Lee, D.Y. Yoon, B.K. Song, "Lipase-catalyzed synthesis of glycerol carbonate from renewable glycerol and dimethyl carbonate through transesterification", *J. Mol. Catal. B: Enzyme* 49 (2007) 75–78.
- [24]. J.R. Ochoa-Gómez, O. Gómez-Jiménez-Aberasturi, C. Ramírez-López, M. Belsué, "A brief review on industrial alternatives for the manufacturing of glycerol carbonate, a green chemical", *Org. Process Res. Dev.* 16 (2012) 389–399.
- [25]. M.M. Du, Q.X. Li, W.T. Dong, T. Geng, Y.J. Jiang, "Synthesis of glycerol carbonate from glycerol and dimethyl carbonate catalyzed by  $\text{K}_2\text{CO}_3/\text{MgO}$ ", *Res. Chem. In termed.* 38 (2012) 1069–1077.
- [26]. F.S.H. Simanjuntak, T.K. Kim, S.D. Lee, B.S. Ahn, H.S. Kim, H. Lee, CaO-catalyzed synthesis of glycerol carbonate from glycerol and dimethyl carbonate: isolation and characterization of an active Ca species, *Appl. Catal. A: Gen.* 401 (2011) 220–225.
- [27]. M.G. Alvarez, A.M. Segarra, S. Contreras, J.E. Sueiras, F. Medina, F. Figueras, Enhanced use of renewable resources: transesterification of glycerol catalyzed by hydrotalcite-like compounds, *Chem. Eng. J.* 161 (2010) 340–345.
- [28]. Pengfei Lu, Huajun Wang, Keke Hu., "Synthesis of glycerol carbonate from glycerol and dimethyl carbonate over the extruded CaO-based catalyst", *Chemical Engineering Journal* 228 (2013) 147–154.
- [29]. S. Sato, F. Sato, H. Gotoh, Y. Yamada, "Selective Dehydration of Alkanediols into Unsaturated Alcohols over Rare Earth Oxide Catalysts", *ACS Catal.* 3 (2013) 721–734.
- [30]. Kankanit Phiw dang, Sineenart Suphankij, Wanichaya Mekprasart and Wisanu Pecharapa, "Synthesis of CuO Nanoparticles by Precipitation Method Using Different Precursors", *Energy Procedia* 34 ( 2013 ) 740 – 745.

- [31]. Jun-Gill Kang, Young-II Kim, Dae Won Cho, Young ku Sohn, “Synthesis and physicochemical properties of  $\text{La}(\text{OH})_3$  and  $\text{La}_2\text{O}_3$  nanostructures”, *Materials Science in Semiconductor Processing* 40 (2015) 737–743.
- [32] T. Miwa, S. Kaneco, H. Katsumata, T. Suzuki, K. Onta, S.C. Verma, K. Sugihara, Photocatalytic hydrogen production from aqueous methanol solution with  $\text{CuO}/\text{Al}_2\text{O}_3/\text{TiO}_2$  nanocomposite, *Int. J. Hydrog. Energy*, 35 (2010) 6554-6560.
- [33] M. Bahmani, B.V. Farahani, S. Sahebdehfar, Preparation of high performance nano-sized  $\text{Cu}/\text{ZnO}/\text{Al}_2\text{O}_3$  methanol synthesis catalyst via aluminum hydrous oxide sol, *Appl. Catal. A: Gen.* 520 (2016) 178-187.
- [34] S. Paulose, R. Raghavan, B.K. George, Copper oxide alumina composite via template assisted sol-gel method for ammonium perchlorate decomposition, *J. Ind. Eng. Chem.* 53 (2017) 155-163.
- [35] R. Shokrani, M. Haghghi, N. Jodeiri, H. Ajamein, M. Abdollahifar, Fuel cell grade hydrogen production via methanol steam reforming over  $\text{CuO}/\text{ZnO}/\text{Al}_2\text{O}_3$  nanocatalyst with various oxide ratios synthesized via urea-nitrates combustion method, *Int. J. Hydrog. Energy*, 39 (2014) 13141-13155.
- [36]. A.J. Parker, Q. Rev, “The effects of solvation on the properties of anions in dipolar aprotic solvents”, *Chem. Soc.* 16 (1962) 163–187.
- [37]. A. Kordikowski, A.P. Schenk, R.M. Van Nielen, C.J. Peters, J. Supercrit. Fluids, 1995 “Volume expansions and vapor-liquid equilibria of binary mixtures of a variety of polar solvents and certain near-critical solvents” 8(1995) 205–216.
- [38]. J. Robert, W. Stevens, R. V. Siriwardane and J. Logan, “In Situ Fourier Transform Infrared (FTIR) Investigation of  $\text{CO}_2$  Adsorption onto Zeolite Materials”, *Energy Fuels*, 2008(5), 22, 3070– 3079.
- [39]. M. León, E. Díaz, S. Bennici, A. Vega, S. Ordóñez and A. Auroux, “Adsorption of  $\text{CO}_2$  on Hydrotalcite-Derived Mixed Oxides: Sorption Mechanisms and Consequences for Adsorption Irreversibility”, *Ind. Eng. Chem. Res.*, 2010, 49(8), 3663–3671.
- [40]. H. Du, C. T. Williams, A. D. Ebner and J. A. Ritter, “In Situ FTIR Spectroscopic Analysis of Carbonate Transformations during Adsorption and Desorption of  $\text{CO}_2$  in K-Promoted HTlc”, *Chem. Mater.*, 2010, 22(11), 3519–3526.
- [41]. C. Hammond, J. A. Lopez-Sanchez, M. H. A. Rahim, N. Dimitratos, R. L. Jenkins, A. F. Carley, Q. He, C. J. Kiely, D. W. Knight and G. J. Hutchings, *Dalton Trans.*, “Synthesis of glycerol carbonate from glycerol and urea with gold-based catalysts”, 2011 Apr 21, 40, 3927–3937.
- [42]. Y. Du, L. He and D. Kong, *Catal. Commun.*, “Magnesium-catalyzed synthesis of organic carbonate from 1,2-diol/alcohol and carbon dioxide”, 2008 20 April , 9, 1754–1758.